EFFECTS OF SMALL BOUNDARY PERTURBATION ON THE MHD DUCT FLOW

Ulavathi Shettar Mahabaleshwar, Igor Pažanin, Marko Radulović, and Francisco Javier Suárez-Grau

ABSTRACT. In this paper, we investigate the effects of small boundary perturbation on the laminar motion of a conducting fluid in a rectangular duct under applied transverse magnetic field. A small boundary perturbation of magnitude ϵ is applied on cross-section of the duct. Using the asymptotic analysis with respect to ϵ, we derive the effective model given by the explicit formulae for the velocity and induced magnetic field. Numerical results are provided confirming that the considered perturbation has nonlocal impact on the asymptotic solution.

1. Introduction

It is well-known that only a limited number of the fluid flow problems can be solved (or approximated) by the solutions in the explicit form. To derive such solutions, we usually need to start with (over)simplified mathematical models and consider ideal geometries on the flow domains with no distortions introduced. However, in practice, the boundary of the fluid domain can contain various small irregularities (rugosities, dents, etc.) being far from the ideal one. Such problems are challenging from the mathematical point of view and, in most cases, can be treated only numerically. The analytical treatments are rare because introducing the small parameter as the perturbation quantity in the domain boundary forces us to perform tedious change of variables. As a result, we obtain the problem that cannot be solved analytically and is only amenable for numerical simulations. Having this in mind, not many analytical results on the subject can be found in the existing literature, both engineering and mathematical. We refer the reader to monograph [1] (and the references therein) for more details on the subject of boundary perturbation in boundary–value problems for PDEs.

In this paper we address the magnetohydrodynamic (MHD) flow of electrically conducting and incompressible liquid through a duct under the action of a trans-

---

verse magnetic field. Such flows naturally appear in the industrial applications, such as nuclear reactors, MHD generators, accelerators, pumps, etc. For that reason, MHD duct problems have been continuously investigated for a long time, starting from the pioneering paper by Hartmann [2] to nowadays. Here we mention only the papers that influenced our work and refer the reader to [3–8].

The goal of this paper is to study the effects of slightly perturbed boundary on the MHD flow through a rectangular duct. More precisely, we assume that the cross-section of the duct has the following form:

$$\hat{\Omega}^\epsilon = \left\{ (\hat{x}, \hat{y}) \in \mathbb{R}^2 : -b < \hat{x} < b, \ -a < \hat{y} < a - \lambda f\left(\frac{\hat{x}}{a}\right) \right\}.$$

The ratio $\epsilon = \frac{\lambda}{a}$ is taken to be a small parameter ($0 < \epsilon \ll 1$), while f is assumed to be an arbitrary smooth function of $\mathcal{O}(1)$ magnitude. For the purpose of our analysis, it is convenient to work in non-dimensional setting so we normalize physical variables by a (see Section 2) and address the MHD flow problem in the domain (see Fig. 1):

$$\Omega^\epsilon = \left\{ (x, y) \in \mathbb{R}^2 : -c < x < c, \ -1 < y < 1 - \epsilon f(x) \right\}, \quad c = \frac{b}{a}.$$
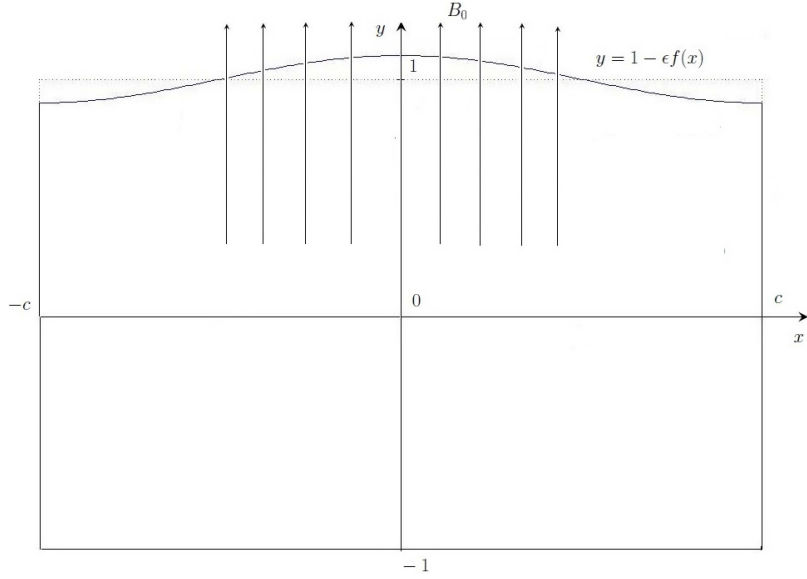

FIGURE 1. Cross-section of a duct after non-dimensionalization.

Due to the strong coupling of the equations of fluid mechanics and electrodynamics, exact solutions can be derived only in case of ideal geometries under simple (physically doubtful) boundary conditions (see e.g. [9]). Here, of course, we cannot hope to do the same, so we employ asymptotic analysis and seek for the approximate solution. Instead of rewriting the governing problem in an ϵ–independent

domain (by introducing the suitable change of variables), we choose different, more efficient approach. It consists of expanding the unknown functions in the Taylor series with respect to y (in the vicinity of the upper boundary) and applying the asymptotic expansion technique (see Section 3). The boundary value problems describing the first two terms in the expansion remain strongly coupled, but we can solve them analytically in case of non-conducting walls parallel to the imposed magnetic field and perfectly conducting walls perpendicular to the field. Employing Fourier series representation of the solution, we derive explicit expressions for the first-order approximation and corresponding corrector. The first-order approximation does not feel the effects of the small boundary perturbation and that was to be expected. The effects we seek for appear in the correctors, as confirmed numerically with many illustrations in Section 4. We use relatively small Hartmann numbers in the process to better illustrate the desired effects, since greater Hartmann numbers lead to solutions having an infinite number of inflexion points. It turns out that the small perturbation of the domain boundary affects the solution not only locally (near the upper boundary), but also (moderately) far from the perturbed boundary and these findings represent our main contribution.

We finish the Introduction by providing additional bibliographic remarks. For fluid flows, the boundary perturbation investigations are mostly done in the context of periodically corrugated boundaries, see e.g. [10–15]. The study not limited to periodic corrugations has been performed recently for classical Newtonian flow [16], micropolar fluid flow [17] and porous medium flow [18]. This work is, in fact, the continuation of this research. The results presented here are valid for an arbitrary (smooth enough) boundary perturbation function f and that should be emphasized. To conclude, though the MHD duct flows have been studied extensively (as mentioned above), the influence of the boundary perturbation on such flows has not been addressed so far, at least to our knowledge. Thus, it is our firm belief that our results will prove useful in the engineering practice, in particular in those industrial applications where the MHD flow is affected by the wall roughness.

2. The equations and boundary conditions

We study the stationary flow of an incompressible conducting fluid governed by a pressure gradient along a duct, under an applied transverse magnetic field. We suppose that no secondary flow is produced and that there are no variations in the duct cross-section or imposed magnetic field with distance z along the duct. As a consequence, all physical quantities except pressure are constant along the duct (i.e. independent of z). Finally, we assume that the induced magnetic field due to the motion of the fluid does not disturb the applied magnetic field so the latter can be taken as the constant field of flux density B_0 in y-direction. In view of that, the classical Maxwell equations reduce to (see e.g. [4] for details):

$$(2.1) \qquad \mu\left(\frac{\partial^2 \hat{u}_z^\epsilon}{\partial \hat{x}^2} + \frac{\partial^2 \hat{u}_z^\epsilon}{\partial \hat{y}^2}\right) + B_0 \frac{\partial \hat{H}_z^\epsilon}{\partial \hat{y}} - \frac{\partial \hat{p}^\epsilon}{\partial z} = 0, \qquad \text{in } \hat{\Omega}^\epsilon,$$

$$(2.2) \qquad \frac{1}{\sigma}\left(\frac{\partial^2 \hat{H}_z^\epsilon}{\partial \hat{x}^2} + \frac{\partial^2 \hat{H}_z^\epsilon}{\partial \hat{y}^2}\right) + B_0 \frac{\partial \hat{u}_z^\epsilon}{\partial y} = 0, \qquad \text{in } \hat{\Omega}^\epsilon.$$

In the above system, the unknowns are the fluid velocity $\hat{u}_z^\epsilon$ and the induced magnetic field $\hat{H}_z^\epsilon$. The superscript ϵ is added into the notation to stress the dependence of the solution on the small parameter as well. We denote by σ, μ and $\frac{\partial \hat{p}^\epsilon}{\partial z}$ the constant conductivity, viscosity of the fluid and pressure gradient, respectively. The above equations should be endowed with the appropriate boundary conditions. As indicated in the Introduction, we impose:

$$(2.3) \qquad \hat{u}_z^\epsilon = 0, \qquad \frac{\partial \hat{H}_z^\epsilon}{\partial \hat{y}} = 0, \qquad \text{for } \hat{y} = -a, a - \lambda f\left(\frac{\hat{x}}{a}\right),$$

$$(2.4) \qquad \hat{u}_z^\epsilon = 0, \qquad \hat{H}_z^\epsilon = 0, \qquad \text{for } \hat{x} = -b, b,$$

meaning that we have non–conducting walls parallel to the applied magnetic field and perfectly conducting walls perpendicular to the field.

Let us rewrite the problem (2.1)–(2.4) in dimensionless form. To accomplish that, we introduce:

$$x = \frac{\hat{x}}{b}, \qquad y = \frac{\hat{y}}{a}, \qquad M = aB_0\sqrt{\frac{\sigma}{\mu}}, \qquad c = \frac{b}{a}, \qquad \epsilon = \frac{\lambda}{a},$$

$$u^\epsilon = \frac{\mu \hat{u}_z^\epsilon}{a^2(-\frac{\partial \hat{p}^\epsilon}{\partial z})}, \qquad H^\epsilon = \sqrt{\frac{\mu}{\sigma}} \frac{\hat{H}_z^\epsilon}{(-\frac{\partial \hat{p}^\epsilon}{\partial z})a^2}.$$

In view of that, the problem under consideration becomes:

$$(2.5) \qquad \frac{\partial^2 u^\epsilon}{\partial x^2} + \frac{\partial^2 u^\epsilon}{\partial y^2} + M\frac{\partial H^\epsilon}{\partial y} = -1, \qquad \text{in } \Omega^\epsilon,$$

$$(2.6) \qquad \frac{\partial^2 H^\epsilon}{\partial x^2} + \frac{\partial^2 H^\epsilon}{\partial y^2} + M\frac{\partial u^\epsilon}{\partial y} = 0, \qquad \text{in } \Omega^\epsilon,$$

with the boundary conditions

$$(2.7) \qquad u^\epsilon = 0, \qquad \frac{\partial H^\epsilon}{\partial y} = 0, \qquad \text{for } y = -1, 1 - \epsilon f(x),$$

$$(2.8) \qquad u^\epsilon = 0, \qquad H^\epsilon = 0, \qquad \text{for } x = -c, c.$$

Note that a non-dimensional parameter M (Hartmann number) appears in the dimensionless equations depending on the flux density, fluid viscosity and conductivity. Its order of magnitude could be very important in practical applications. Our goal is to investigate the effective behaviour of the flow governed by (2.5)–(2.8), as $\epsilon \to 0$.

3. Asymptotic analysis

To keep the notation as simple as possible, in the following we assume that $f < 0$. By doing that, we have $\Omega = \{(x,y) \in \mathbb{R}^2 : -c < x < c, -1 < y < 1\} \subset \Omega^\epsilon$ so that the solution (u^ϵ, H^ϵ) of (2.5)–(2.8) is defined on Ω. As a consequence, we are in position to directly expand velocity in Taylor series with respect to y near the upper boundary (otherwise, we would have to extend the solution to Ω and contaminate the notation). Before, proceeding, it must be emphasized that this is just a technical assumption, i.e. the obtained results are valid for an arbitrary

(smooth enough) function f. That is essentially due to the fact that it can be proved that the approximation derived in the sequel is asymptotically the same as the one that could be built if we have first passed to the ϵ-independent domain by introducing the change of variable, namely $z = \frac{y}{1-\epsilon h}$. This part is straightforward and can be done following the same procedure as in [16, 18].

We expand as follows:

$$u^\epsilon(x,y) = \sum_{k=0}^{\infty} \frac{1}{k!} \frac{\partial^k u^\epsilon}{\partial y^k}(x,1)(y-1)^k, \qquad H^\epsilon(x,y) = \sum_{k=0}^{\infty} \frac{1}{k!} \frac{\partial^k H^\epsilon}{\partial y^k}(x,1)(y-1)^k.$$

In view of the boundary conditions (2.7), we deduce

$$(3.1) \quad 0 = u^\epsilon(x, 1-\epsilon f) = u^\epsilon(x,1) - \epsilon f(x)\frac{\partial u^\epsilon}{\partial y}(x,1) + \frac{\epsilon^2}{2}f(x)^2\frac{\partial^2 u^\epsilon}{\partial y^2}(x,1) - \ldots,$$

$$(3.2) \quad 0 = \frac{\partial H^\epsilon}{\partial y}(x,1-\epsilon f) = \frac{\partial H^\epsilon}{\partial y}(x,1) - \epsilon f(x)\frac{\partial^2 H^\epsilon}{\partial y^2}(x,1)$$
$$+ \frac{\epsilon^2}{2}f(x)^2\frac{\partial^3 H^\epsilon}{\partial y^3}(x,1) - \ldots.$$

On the other hand, we seek for the unknowns in the form of the asymptotic expansion in powers of ϵ:

$$(3.3) \quad \begin{aligned} u^\epsilon(x,y) &= u^0(x,y) + \epsilon u^1(x,y) + \epsilon^2 u^2(x,y) + \ldots, \\ H^\epsilon(x,y) &= H^0(x,y) + \epsilon H^1(x,y) + \epsilon^2 H^2(x,y) + \ldots \end{aligned}$$

Plugging the above expansions (3.3) into (3.1)–(3.2) yields

$$0 = u^0(x,1) + \epsilon\left(u^1(x,1) - f(x)\frac{\partial u^0}{\partial y}(x,1)\right)$$
$$+ \epsilon^2\left(u^2(x,1) - f(x)\frac{\partial u^1}{\partial y}(x,1) + \frac{f(x)^2}{2}\frac{\partial^2 u^0}{\partial y^2}(x,1)\right) + \ldots,$$

$$0 = \frac{\partial H^0}{\partial y}(x,1) + \epsilon\left(\frac{\partial H^1}{\partial y}(x,1) - f(x)\frac{\partial^2 H^0}{\partial^2 y}(x,1)\right)$$
$$+ \epsilon^2\left(\frac{\partial H^2}{\partial y}(x,1) - f(x)\frac{\partial^2 H^1}{\partial y^2}(x,1) + \frac{f(x)^2}{2}\frac{\partial^3 H^0}{\partial y^3}(x,1)\right) + \ldots.$$

As a result, we obtain the effective boundary conditions satisfied by the first two terms at the upper boundary:

$$u^0(x,1) = 0, \qquad\qquad \frac{\partial H^0}{\partial y}(x,1) = 0,$$

$$u^1(x,1) = f(x)\frac{\partial u^0}{\partial y}(x,1), \qquad\qquad \frac{\partial H^1}{\partial y}(x,1) = f(x)\frac{\partial^2 H^0}{\partial y^2}(x,1).$$

3.1. First-order approximation. The first-order approximation (u^0, H^0) satisfies the following system:

$$(3.4) \qquad \frac{\partial u^0}{\partial x^2} + \frac{\partial^2 u^0}{\partial y^2} + M\frac{\partial H^0}{\partial y} = -1, \qquad\qquad \text{in } \Omega,$$

$$(3.5) \qquad \frac{\partial^2 H^0}{\partial x^2} + \frac{\partial^2 H^0}{\partial y^2} + M\frac{\partial u^0}{\partial y} = 0, \qquad\qquad \text{in } \Omega,$$

equipped with the boundary conditions

$$(3.6) \quad u^0(x,-1) = 0, \quad u^0(x,1) = 0, \quad \frac{\partial H^0}{\partial y}(x,-1) = 0, \quad \frac{\partial H^0}{\partial y}(x,1) = 0,$$

$$(3.7) \quad u^0(-c,y) = 0, \quad u^0(c,y) = 0, \quad H^0(-c,y) = 0, \quad H^0(c,y) = 0.$$

We note that the above problem is strongly coupled. Following [4], we can solve it by seeking the solution in the form of the Fourier cosine series, namely:

$$(3.8) \qquad u^0(x,y) = \sum_{k=0}^{\infty} v_k(y) \cos\left(\frac{(k+\frac{1}{2})\pi}{c}x\right),$$

$$(3.9) \qquad H^0(x,y) = \sum_{k=0}^{\infty} h_k(y) \cos\left(\frac{(k+\frac{1}{2})\pi}{c}x\right).$$

Observe that (3.8)–(3.9) are postulated in a way so that the boundary conditions (3.7) are automatically fulfilled.

REMARK 3.1. Taking into account the practical applications, it would be even more of interest to analyze the case of the rectangular duct with perfectly conducting walls parallel to the imposed magnetic field and non-conducting walls perpendicular to the field. The boundary conditions in that case read:

$$u^\epsilon = 0, \qquad\qquad H^\epsilon = 0, \qquad\qquad \text{for } y = -1, 1 - \epsilon f(x),$$

$$u^\epsilon = 0, \qquad\qquad \frac{\partial H^\epsilon}{\partial x} = 0, \qquad\qquad \text{for } x = -c, c.$$

By following the above procedure, we would arrive to the conclusion that the system (3.4)–(3.5) cannot be solved in order to meet the zero boundary conditions for the velocity at $x = -c, c$. It means that the boundary layers appear in the vicinity of $x = -c, c$ forcing us to change the approach. This is the subject of our current investigation. Formal analysis of the boundary layers in this case has been carried out in [5] for high Hartman numbers and with no boundary distortions introduced.

In the sequel, we use the representation

$$(3.10) \qquad\qquad 1 = \sum_{k=0}^{\infty} a_k \cos\left(\frac{(k+\frac{1}{2})\pi}{c}x\right),$$

where

$$(3.11) \qquad a_k = \frac{1}{c}\int_{-c}^{c} \cos\left(\frac{(k+\frac{1}{2})\pi}{c}x\right)dx = \frac{2\cdot(-1)^k}{(k+\frac{1}{2})\pi}.$$

Substituting (3.8)–(3.9), (3.10)–(3.11) into the equations (3.4)–(3.5), we get a second-order system of ODEs satisfied by v_k, h_k and a_k, namely:

$$(3.12) \qquad v_k'' - \alpha_k^2 v_k + M h_k' = -a_k,$$

$$(3.13) \qquad h_k'' - \alpha_k^2 h_k + M v_k' = 0,$$

with $\alpha_k = \frac{(k+\frac{1}{2})\pi}{c}$. Let us solve (3.12)–(3.13). Differentiating (3.12), we obtain the following equation

$$(3.14) \qquad v_k''' - \alpha_k^2 v_k' + M h_k'' = 0.$$

Multiplying (3.13) by the Hartmann number M and then subtracting the obtained equation from (3.14), we get

$$v_k''' - (\alpha_k^2 + M^2) v_k' + \alpha_k^2 M h_k = 0$$

implying

$$(3.15) \qquad h_k = \frac{1}{\alpha_k^2 M}(-v_k''' + (\alpha_k^2 + M^2) v_k').$$

Now, from (3.12) and (3.15) we deduce the equation for v_k

$$v_k^{(4)} - (2\alpha_k^2 + M^2) v_k'' + \alpha_k^4 v_k = \alpha_k^2 a_k.$$

We can easily solve it leading to

$$(3.16) \qquad v_k(y) = V_k^1 \sinh(r_{1k}y) + V_k^2 \cosh(r_{1k}y) + V_k^3 \sinh(r_{2k}y)$$
$$+ V_k^4 \cosh(r_{2k}y) + \frac{1}{\alpha_k^2} a_k,$$

where $r_{1k}, r_{2k} = \left[\frac{1}{2}\left(2\alpha_k^2 + M^2 \pm M\sqrt{4\alpha_k^2 + M^2}\right)\right]^{1/2}$. Finally, plugging the equation (3.16) into the relation (3.15) gives

$$(3.17) \qquad h_k(y) = V_k^1 \left(\frac{r_{1k}(\alpha_k^2 + M^2) - r_{1k}^3}{\alpha_k^2 M}\right) \cosh(r_{1k}y)$$
$$+ V_k^2 \left(\frac{r_{1k}(\alpha_k^2 + M^2) - r_{1k}^3}{\alpha_k^2 M}\right) \sinh(r_{1k}y)$$
$$+ V_k^3 \left(\frac{r_{2k}(\alpha_k^2 + M^2) - r_{2k}^3}{\alpha_k^2 M}\right) \cosh(r_{2k}y)$$
$$+ V_k^4 \left(\frac{r_{2k}(\alpha_k^2 + M^2) - r_{2k}^3}{\alpha_k^2 M}\right) \sinh(r_{2k}y).$$

From the boundary conditions (3.6) and Fourier representations (3.8)–(3.9) we deduce the boundary conditions for v_k and h_k:

$$u^0(x, -1) = 0 \ \Rightarrow \ v_k(-1) = 0,$$
$$u^0(x, 1) = 0 \ \Rightarrow \ v_k(1) = 0,$$
$$\frac{\partial H^0}{\partial y}(x, -1) = 0 \ \Rightarrow \ h_k'(-1) = 0,$$

$$\frac{\partial H^0}{\partial y}(x,1) = 0 \;\Rightarrow\; h_k'(1) = 0.$$

Consequently, we determine the constants V_k^l, $l = 1, 2, 3, 4$ as

(3.18)
$$V_k^1 = 0,$$
$$V_k^2 = \frac{a_k r_{2k} B_k}{\alpha_k^2 r_{1k} A_k \cosh(r_{1k})\left(1 - \frac{r_{2k} B_k}{r_{1k} A_k}\right)},$$
$$V_k^3 = 0,$$
$$V_k^4 = -\frac{a_k}{\alpha_k^2 \cosh(r_{2k})\left(1 - \frac{r_{2k} B_k}{r_{1k} A_k}\right)},$$

with $A_k = \frac{r_{1k}(\alpha_k^2 + M^2) - r_{1k}^3}{\alpha_k^2 M}$ and $B_k = \frac{r_{2k}(\alpha_k^2 + M^2) - r_{2k}^3}{\alpha_k^2 M}$. To conclude, our first-order approximation reads

(3.19)
$$u^0(x,y) = \sum_{k=0}^{\infty} v_k(y) \cos\left(\frac{(k + \frac{1}{2})\pi}{c} x\right),$$
$$H^0(x,y) = \sum_{k=0}^{\infty} h_k(y) \cos\left(\frac{(k + \frac{1}{2})\pi}{c} x\right),$$

where $v_k(y)$ and $h_k(y)$ are given by (3.16)–(3.17) and the constants V_k^l are provided with (3.18).

3.2. Correctors. As expected, no effects of the boundary perturbation can be seen from the first order approximation (3.19). Thus, we continue the computation by identifying the next term in the asymptotic expansions (3.3). The problem satisfied by the corrector (u^1, H^1) reads as follows:

$$\frac{\partial^2 u^1}{\partial x^2} + \frac{\partial^2 u^1}{\partial y^2} + M\frac{\partial H^1}{\partial y} = -1, \qquad \text{in } \Omega,$$
$$\frac{\partial^2 H^1}{\partial x^2} + \frac{\partial^2 H^1}{\partial y^2} + M\frac{\partial u^1}{\partial y} = 0, \qquad \text{in } \Omega,$$

with

(3.20)
$$u^0(x, -1) = 0, \quad u^1(x, 1) = f(x)\frac{\partial u^0}{\partial y}(x, 1),$$

(3.21)
$$\frac{\partial H^1}{\partial y}(x, -1) = 0, \quad \frac{\partial H^1}{\partial y}(x, 1) = f(x)\frac{\partial^2 H^0}{\partial y^2}(x, 1),$$

(3.22)
$$u^1(-c, y) = 0, \quad u^1(c, y) = 0, \quad H^1(-c, y) = 0, \quad u^1(c, y) = 0.$$

We notice that the perturbation function $f(x)$ now appears in the boundary conditions (3.20)–(3.21) carrying the effects we seek for. We again represent the solution in the form of the Fourier cosine series:

$$u^1(x,y) = \sum_{k=0}^{\infty} w_k(y) \cos\left(\frac{(k + \frac{1}{2})\pi}{c} x\right),$$

$$H^1(x,y) = \sum_{k=0}^{\infty} d_k(y) \cos\left(\frac{(k+\frac{1}{2})\pi}{c} x\right).$$

Consequently, the boundary conditions (3.22) are automatically satisfied and, as in Section 3.1, we get

$$(3.23) \qquad w_k(y) = W_k^1 \sinh(r_{1k}y) + W_k^2 \cosh(r_{1k}y) + W_k^3 \sinh(r_{2k}y)$$
$$+ W_k^4 \cosh(r_{2k}y) + \frac{1}{\alpha_k^2} a_k,$$

$$(3.24) \qquad \begin{aligned} d_k(y) = W_k^1 &\left(\frac{r_{1k}(\alpha_k^2 + M^2) - r_{1k}^3}{\alpha_k^2 M}\right) \cosh(r_{1k}y) \\ + W_k^2 &\left(\frac{r_{1k}(\alpha_k^2 + M^2) - r_{1k}^3}{\alpha_k^2 M}\right) \sinh(r_{1k}y) \\ + W_k^3 &\left(\frac{r_{2k}(\alpha_k^2 + M^2) - r_{2k}^3}{\alpha_k^2 M}\right) \cosh(r_{2k}y) \\ + W_k^4 &\left(\frac{r_{2k}(\alpha_k^2 + M^2) - r_{2k}^3}{\alpha_k^2 M}\right) \sinh(r_{2k}y). \end{aligned}$$

From $(3.20)_1$ and $(3.21)_1$, we deduce

$$(3.25) \qquad w_k(-1) = 0, \quad d_k'(-1) = 0,$$

while for the upper boundary we have (see $(3.20)_2$, $(3.21)_2$)

$$(3.26) \qquad \sum_{k=0}^{\infty} w_k(1) \cos\left(\frac{(k+\frac{1}{2})\pi}{c} x\right) = f(x) \sum_{i=0}^{\infty} v_i'(1) \cos\left(\frac{(k+\frac{1}{2})\pi}{c} x\right),$$

$$(3.27) \qquad \sum_{k=0}^{\infty} d_k'(1) \cos\left(\frac{(k+\frac{1}{2})\pi}{c} x\right) = f(x) \sum_{i=0}^{\infty} h_i''(1) \cos\left(\frac{(k+\frac{1}{2})\pi}{c} x\right).$$

Since we will use finite series approximations in the numerical simulations, we can consider a finite number of terms in (3.26) and proceed as follows:

$$\sum_{k=0}^{n} w_k(1) \cos\left(\frac{(k+\frac{1}{2})\pi}{c} x\right) = \sum_{i=0}^{n} v_i'(1) f(x) \cos\left(\frac{(i+\frac{1}{2})\pi}{c} x\right).$$

Multiplying the above equation with $\cos\left(\frac{(j+\frac{1}{2})\pi}{c} x\right)$, integrating with respect to x, and taking into account that

$$\int_{-c}^{c} \cos\left(\frac{(k+\frac{1}{2})\pi}{c} x\right) \cos\left(\frac{(j+\frac{1}{2})\pi}{c} x\right) dx = \begin{cases} c, & j = k, \\ 0, & j \neq k, \end{cases}$$

we obtain

$$(3.28) \qquad w_k(1) = \frac{1}{c} \sum_{i=0}^{n} v_i'(1) \int_{-c}^{c} f(x) \cos\left(\frac{(i+\frac{1}{2})\pi}{c} x\right) \cos\left(\frac{(k+\frac{1}{2})\pi}{c} x\right) dx.$$

Analogously, from (3.27) we conclude

$$(3.29) \qquad d'_k(1) = \frac{1}{c} \sum_{i=0}^{m} h''_i(1) \int_{-c}^{c} f(x) \cos\left(\frac{(i+\frac{1}{2})\pi}{c}x\right) \cos\left(\frac{(k+\frac{1}{2})\pi}{c}x\right) dx.$$

Now, it remains to compute the constants W_k^l, $l = 1, 2, 3, 4$ appearing in (3.23)–(3.24). We do that by taking into account the boundary conditions (3.25), (3.28)–(3.29) leading to

$$(3.30) \qquad \begin{aligned} W_k^1 &= \frac{\frac{1}{2}w_k(1) - W_k^3 \sinh(r_{2k})}{\sinh(r_{1k})}, \\ W_k^2 &= \frac{\frac{1}{2}w_k(1) - \frac{a_k}{\alpha_k^2} - W_k^4 \cosh(r_{2k})}{\cosh(r_{1k})}, \\ W_k^3 &= \frac{d'_k(1) - A_k w_k(1) r_{1k}}{2\sinh(r_{2k})(B_k r_{2k} - A_k r_{1k})}, \\ W_k^4 &= \frac{d'_k(1) - A_k w_k(1) r_{1k} + 2\frac{a_k}{\alpha_k^2} A_k r_{1k}}{2\cosh(r_{2k})(B_k r_{2k} - A_k r_{1k})}, \end{aligned}$$

where $A_k = \frac{r_{1k}(\alpha_k^2 + M^2) - r_{1k}^3}{\alpha_k^2 M}$ and $B_k = \frac{r_{2k}(\alpha_k^2 + M^2) - r_{2k}^3}{\alpha_k^2 M}$. Thus, the computed correctors can be written in the following form:

$$(3.31) \qquad u^1(x,y) = \sum_{k=0}^{n} w_k(y) \cos\left(\frac{(k+\frac{1}{2})\pi}{c}x\right),$$

$$H^1(x,y) = \sum_{k=0}^{m} d_k(y) \cos\left(\frac{(k+\frac{1}{2})\pi}{c}x\right),$$

with $w_k(y)$, $d_k(y)$ and W_k^l given by (3.23), (3.24) and (3.30) respectively.

3.3. Asymptotic approximation. To conclude this Section, we define our asymptotic approximation as

$$(3.32) \qquad u_{\text{approx}}^\epsilon(x,y) = u^0(x,y) + \epsilon u^1(x,y),$$

$$(3.33) \qquad H_{\text{approx}}^\epsilon(x,y) = H^0(x,y) + \epsilon H^1(x,y),$$

where the functions u^0, u^1, H^0, H^1 are provided in Sections 3.1 and 3.2. It is important to emphasize that all those functions have been computed explicitly. The asymptotic solution is affected by the small boundary perturbation and those affects are present in the correctors (u^1, H^1). Thus, it is reasonable to expect that the influence of the boundary perturbation on the effective flow is not just local (i.e., near the upper boundary), in particular if ϵ is not too small. This assertion is going to be confirmed in the following section by providing the numerical example.

4. Numerical illustrations

In this section, we visually present our asymptotic solution in order to indicate how the flow adjusts to the presence of small boundary perturbation. Throughout the section, we employ the boundary perturbation function $f(x) = -\cos\left(\frac{\pi x}{4}\right)$ for

$x \in (-2, 2)$. By considering such restriction of the cosine function, we, in fact, consider the non-periodic boundary perturbation. This is consistent with the fact that our analysis is not limited to a perturbation of a periodic nature.

In the numerical example, we take the Hartmann number $M = 5$. Taking higher Hartmann numbers leads to the solution having an infinite number of inflexion points, which is not easily visualized, so we restrict ourselves to the case of Hartmann numbers of smaller magnitude. We first plot the correctors derived in Section 3.2. We bring the 2D profiles of the velocity and induced magnetic field for fixed values of x and y, together with 3D figures. Then, we visually present the whole asymptotic solution given by (3.32)–(3.33) for different magnitudes of small parameter ϵ, namely $\epsilon \in \{0.1, 0.01\}$. Again, we depict the 3D figures along with 2D profiles for fixed values of x and y. 2D profiles are brought only for $\epsilon = 0.1$, since smaller values of ϵ produce no significant impact on the solution.

First, we visualize the correctors u^1 and H^1 provided by (3.31). We first plot the velocity corrector profiles for fixed values $y = 1.0$ and $x = -1.5, -1.0, 0.0, 1.0, 1.5$ and the solution on the whole domain (see Figures 2–5). We then present the profiles of induced field corrector for fixed values $y = -1.0, 1.0$ and $x = -1.5, -1.0, 0.0, 1.0, 1.5$, with the solution on the whole domain as well (see Figures 6–10). The correctors u^1 and H^1 have been computed up to $n = m = 10$ in the Fourier series approximations, since increasing those indexes leads to no significant improvements. The coefficients $w_k(1)$ and $d'_k(1)$ (given by (3.28) and (3.29)) have been calculated using the numerical integration in MATLAB. One can deduce from the scale and shape of the correctors that they contain the effect of the boundary perturbation, being significant near the perturbed boundary $y = 1$ and also present to some extent in the whole domain.
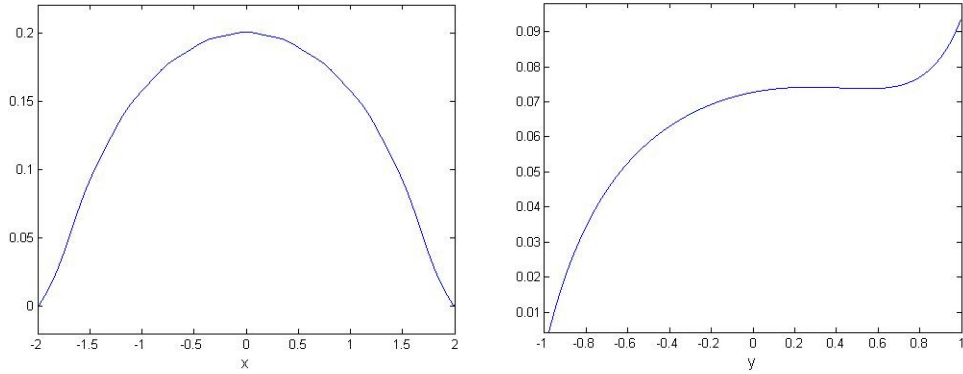
FIGURE 2. The profile of u^1 for fixed $y = 1$ (left) and $x = -1.5$ (right).
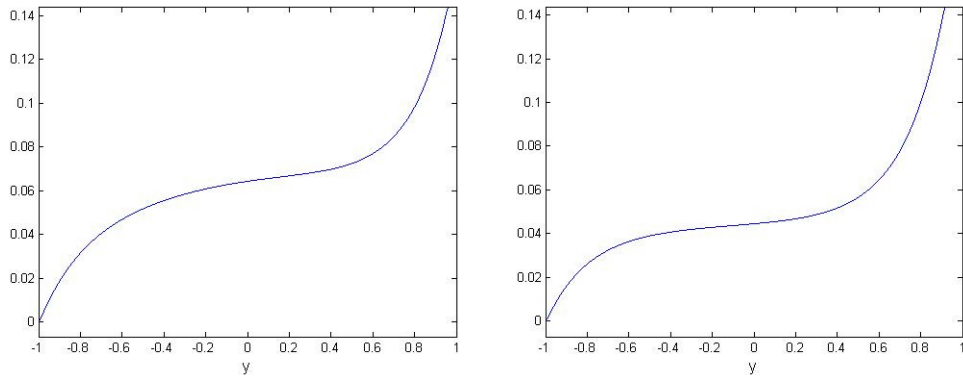
FIGURE 3. The profile of u^1 for fixed $x = -1.0$ (left) and $x = 0.0$ (right).
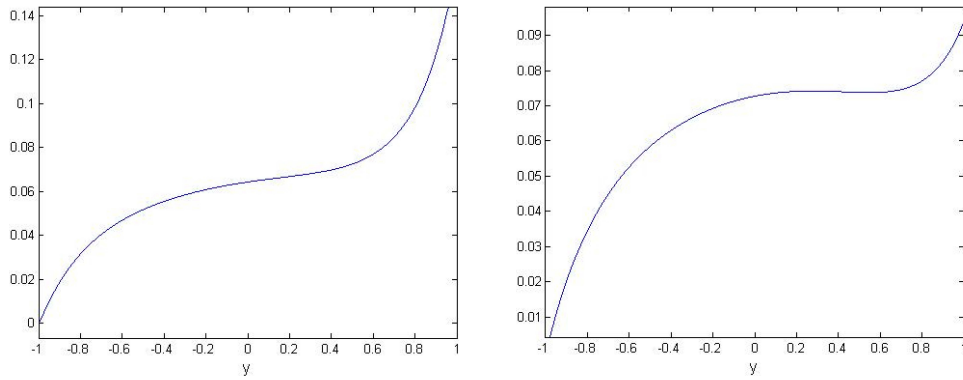
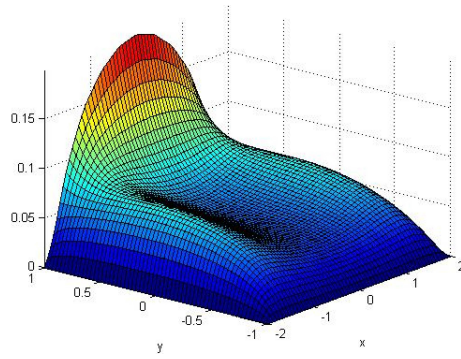FIGURE 4. The profile of u^1 for fixed $x = 1.0$ (left) and $x = 1.5$ (right).
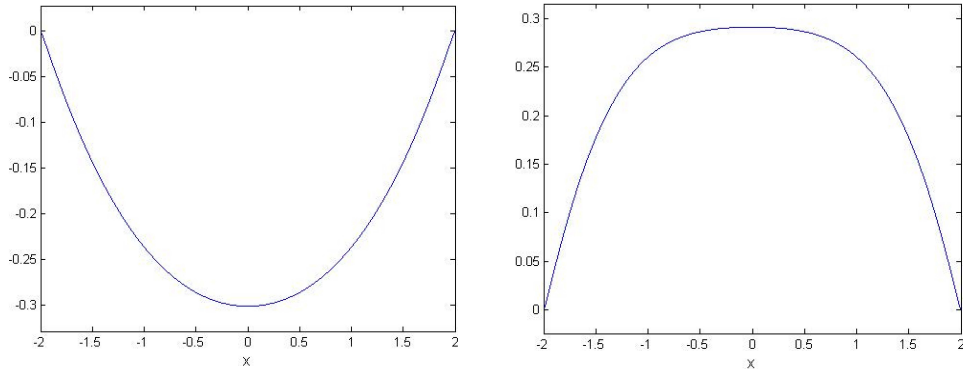

FIGURE 5. The corrector u^1.

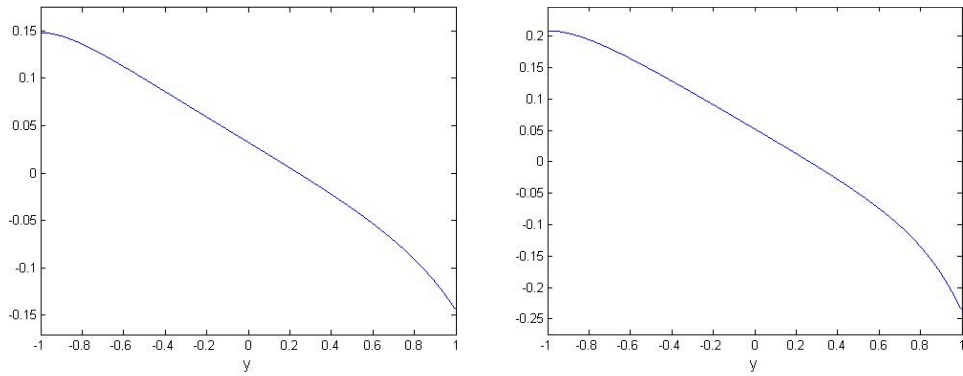FIGURE 6. The profile of H^1 for fixed $y = 1$ (left) and $y = -1$ (right).

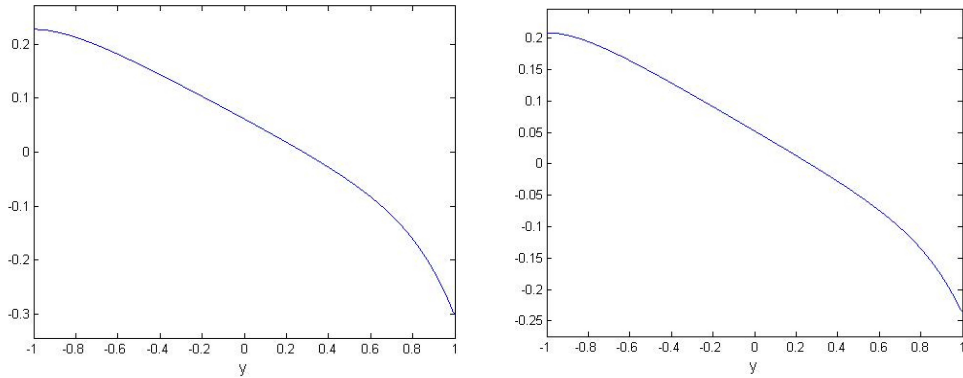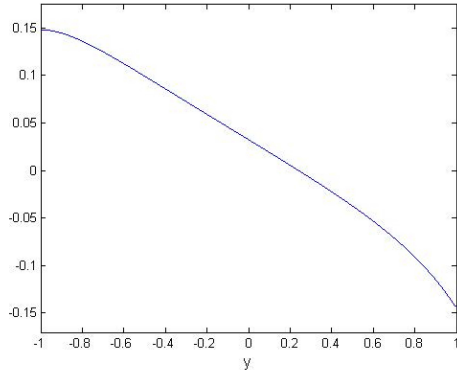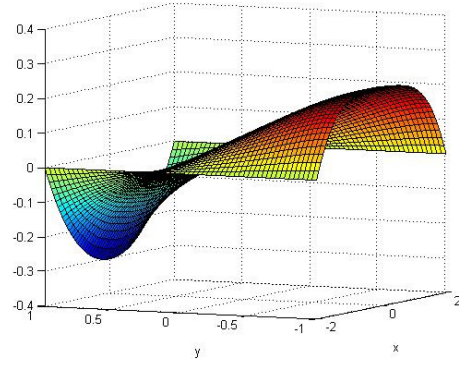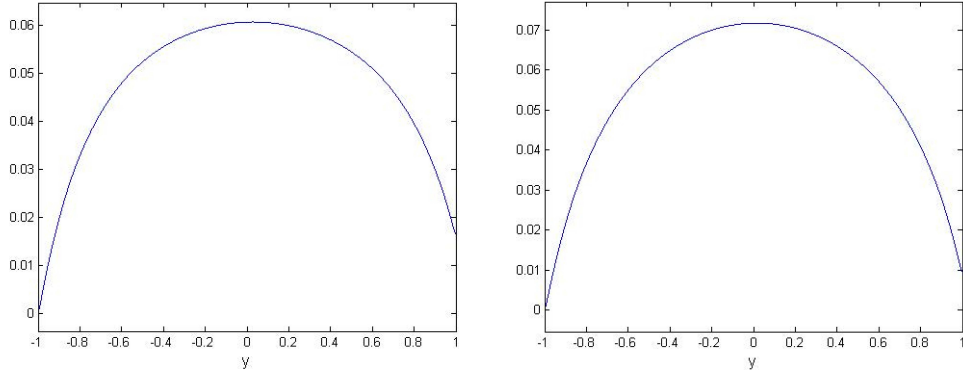FIGURE 7. The profile of H^1 for fixed $x = -1.5$ (left) and $x = -1.0$ (right).

FIGURE 8. The profile of H^1 for fixed $x = 0.0$ (left) and $x = 1.0$ (right).

FIGURE 9. The profile of H^1 for fixed $x = 1.5$.

FIGURE 10. The corrector H^1.
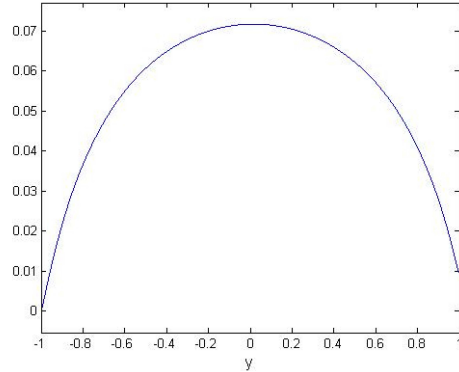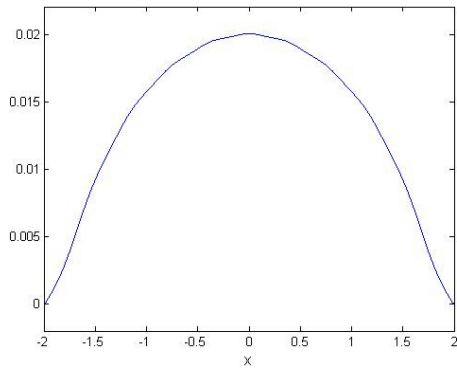
FIGURE 11. The profile of $u_{\mathrm{approx}}^\epsilon$ for fixed $y = 1.0$ (left) and $x = -1.5$ (right).
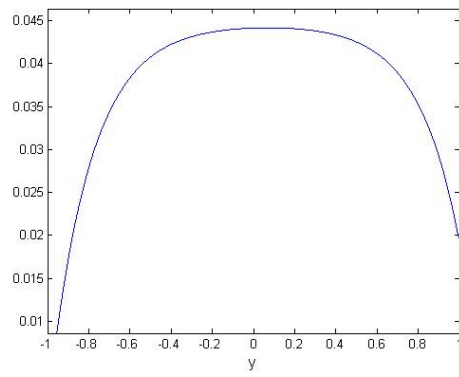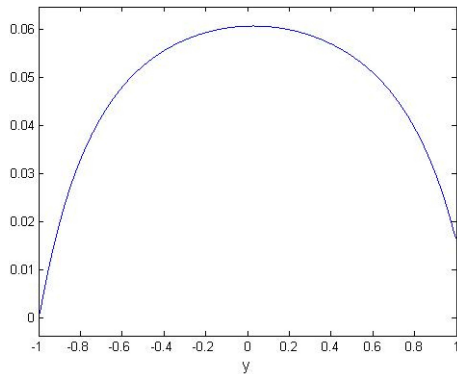
FIGURE 12. The profile of $u_{\mathrm{approx}}^\epsilon$ for fixed $x = -1.0$ (left) and $x = 0.0$ (right).

FIGURE 13. The profile of $u^\epsilon_{\text{approx}}$ for fixed $x = 1.0$ (left) and $x = 1.5$ (right).
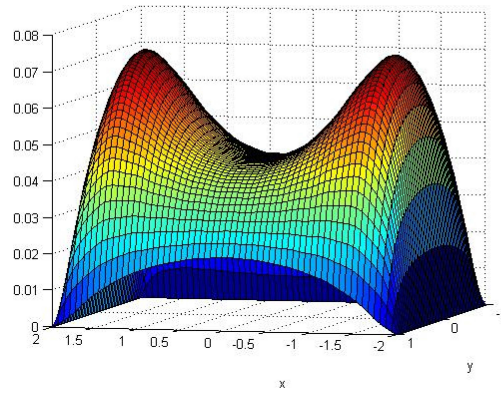

FIGURE 14. Velocity approximation $u^\epsilon_{\text{approx}}$ for $\epsilon = 0.1$.

Then, we present the whole asymptotic approximation given by (3.32)–(3.33). We first depict the velocity approximation profiles for fixed values $y = 1.0$ and $x = -1.5, -1.0, 0.0, 1.0, 1.5$, and the solution on the whole domain for $\epsilon = 0.1$ (see Figures 11–14). Then we plot the profiles of induced magnetic field approximation for fixed values $y = 1.0, -1.0$ and $x = -1.5, -1.0, 0.0, 1.0$, along with the solution on the whole domain for $\epsilon = 0.1$ (see Figures 15–18). We can clearly detect the effects of the boundary perturbation near the upper boundary, and the small, but noticeable impact (moderately) far from the boundary. Lastly, we visualize the velocity and induced field approximation on the whole domain for $\epsilon = 0.01$ (see Figures 19–20). The desired effects for such ϵ turns out to be negligible, so we omit the corresponding 2D profiles.
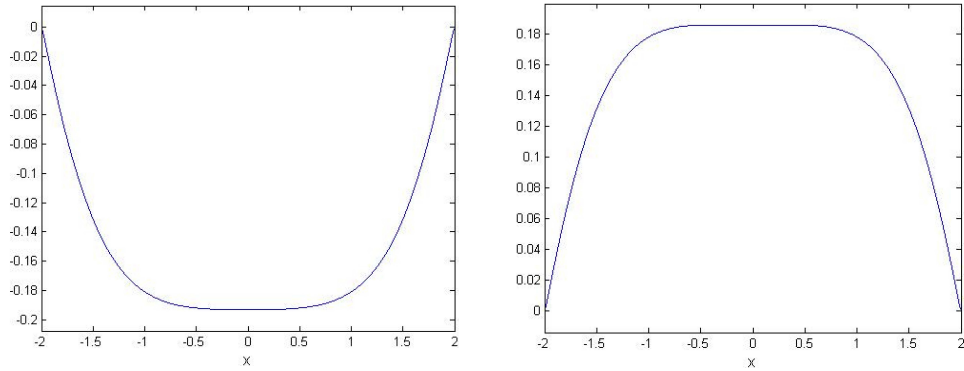
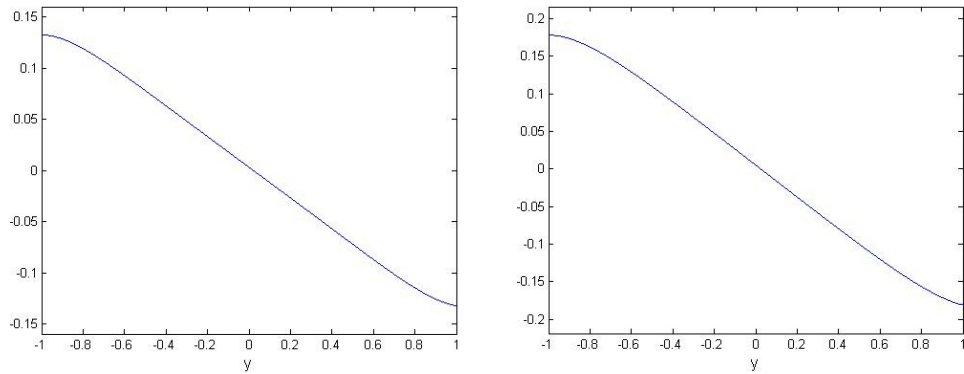FIGURE 15. The profile of $H^\epsilon_{\text{approx}}$ for fixed $y = 1.0$ (left) and $y = -1.0$ (right).

FIGURE 16. The profile of $H^\epsilon_{\text{approx}}$ for fixed $x = -1.5$ (left) and $x = -1.0$ (right).
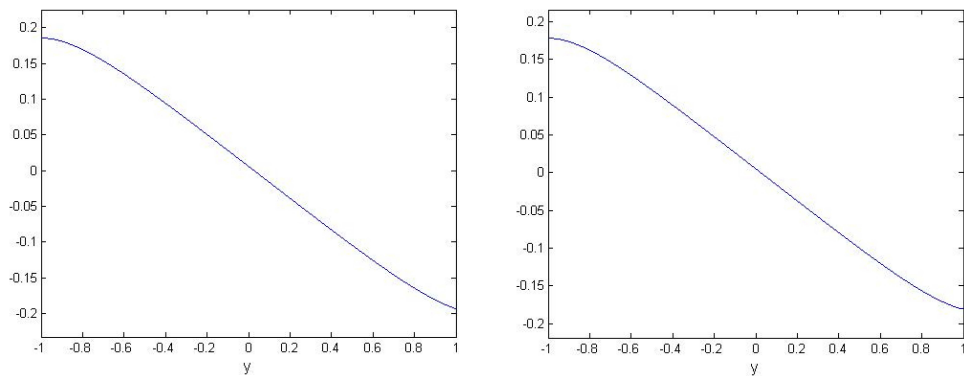

FIGURE 17. The profile of $H^\epsilon_{\text{approx}}$ for fixed $x = 0.0$ (left) and $x = 1.0$ (right).
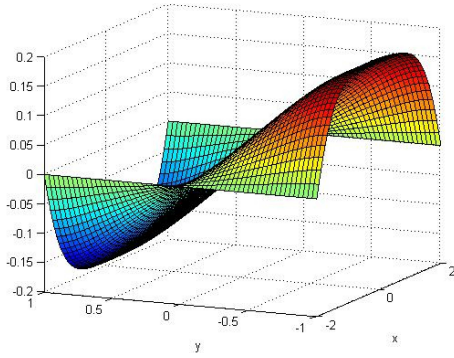
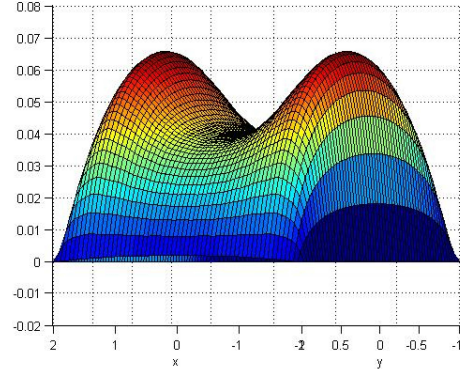FIGURE 18. Induced field approximation $H^\epsilon_{\mathrm{approx}}$ for $\epsilon = 0.1$.

FIGURE 19. Velocity approximation $u^\epsilon_{\mathrm{approx}}$ for $\epsilon = 0.01$.
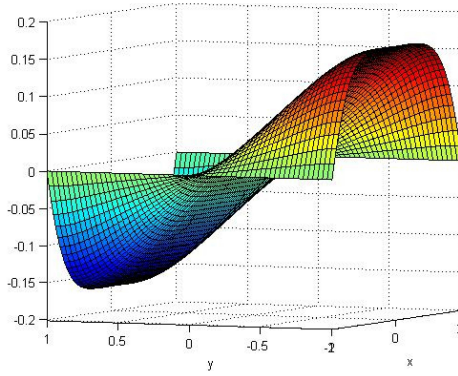

FIGURE 20. Induced field approximation $H^\epsilon_{\mathrm{approx}}$ for $\epsilon = 0.01$.

5. Conclusion

Understanding the effective behavior of the laminar motion of a conducting fluid in a rectangular duct under applied transverse magnetic field is important from the practical point of view because we naturally come across such processes in numerous industrial applications. Since, in practice, the boundary of the fluid domain can contain various small irregularities, it is particularly of interest to study in what way MHD flow is affected by the slightly perturbed boundary. In view of that, in the present paper, we present a formal derivation of the effective model in case of the duct flow flow with non-conducting walls parallel to the imposed magnetic field and perfectly conducting walls perpendicular to the field. The analysis employs a singular perturbation technique and the results are confirmed by the numerical illustrations.

We believe that the result presented here provides a good platform for understanding the influence of small boundary perturbation on the MHD duct flow. The

fact that we have derived the effective system in the form of the explicit formulae for the velocity and induced magnetic field is particularly important with regards to numerical simulations. Since the problem under consideration naturally appears in numerous applications, we hope that the results provided here could have an impact on the current engineering practice. Our further research efforts will be mainly focused on extending the presented analysis on a non-stationary flow, namely to the setting in which the shape function f depends on the time variable as well.

References

1. D. Henry, *Perturbation of the Boundary in Boundary-Value Problems of Partial Differential Equations*, Lond. Math. Soc. Lect. Note Ser. **318**, Cambridge University Press, 2005.
2. J. Hartmann, *Hg-dynamics I: theory of the laminar flow of an electrically conductive liquid in a homogeneous magnetic field*, Mat.-Fys. Medd., K. Dan. Vidensk. Selsk. **15**(6) (1937), 1–28.
3. R. R. Gold, *Magnetohydrodynamic pipe flow. Part 1*, J. Fluid Mech. **13** (1962), 505–512.
4. J. C. R. Hunt, *Magnetohydrodynamic flow in rectangular ducts*, J. Fluid Mech. **21** (1965), 577–590.
5. J. C. R. Hunt, K. Stewartson, *Magnetohydrodynamic flow in rectangular ducts. II*, J. Fluid. Mech. **23** (1965), 563–581.
6. C. Bozkaya, M. Tezer-Sezgin, *Fundamental solution for coupled magnetohydrodynamic flow equations*, J. Comput. Appl. Math. **203** (2007), 125–144.
7. J. V. Ramana Murthy, K. S. Sai, N. K. Bahali, *Steady flow of micropolar fluid in a rectangular channel under transverse magnetic field with suction*, AIP Advances **1**(3) (2011), 032123.
8. T. Zhen, M. Ni, *Analytical solutions for MHD flow at a rectangular duct with unsymmetrical walls of arbitrary conductivity*, Sci. China, Phys. Mech. Astron. **58**(2) (2015), 18p.
9. L. Dragos, *Magneto-Fluid Dynamics*, Abacus Press, England, 1975.
10. Y. Achdou, O. Pironneau, F. Valentin, *Effective boundary conditions for laminar flows over periodic rough boundaries*, J. Comput. Phys. **147** (1998), 187–218.
11. W. Jäger, A. Mikelić, *On the roughness-induced effective boundary conditions for an incompressible viscous flow*, J. Differ. Equations **170** (2001), 96–122.
12. D. Bresch, C. Choquet, L. Chupin, T. Colin, M. Gisclon, *Roughness-induced effect at main order on the Reynolds approximation*, Multiscale Model. Simul. **8** (2010), 997–1017.
13. C-O. Ng, C. Y. Wang, *Darcy-Brinkman flow through a corrugated channel*, Transp. Porous Media **85** (2010), 605–618.
14. D. D. Gray, E. Ogretim, G. S. Bromhal, *Darcy flow in a wavy channel filled with a porous medium*, Transp. Porous Media **98** (2013), 743–753.
15. I. Pažanin, F. J. Suárez-Grau, *Analysis of the thin film flow in a rough thin domain filled with micropolar fluid*, Comput. Math. Appl. **68** (2014), 1915–1932.
16. E. Marušić-Paloka, *Effects of small boundary perturbation on flow of viscous fluid*, ZAMM, Z. Angew. Math. Mech. **96** (2016), 1103–1118.
17. E. Marušić-Paloka, I. Pažanin, M. Radulović, *Flow of a micropolar fluid through a channel with small boundary perturbation*, Z. Naturforsch., A **71** (2016), 607–619.
18. E. Marušić-Paloka, I. Pažanin, *On the Darcy–Brinkman flow through a channel with slightly perturbed boundary*, Transp. Porous Media **117** (2017), 27–44.

ЕФЕКТИ МАЛИХ ПОРЕМЕЋАЈА НА ГРАНИЦИ
МХД ТОКА У КАНАЛУ

У раду испитујемо ефекте малих поремећаја на граници ламинарног тока проводног флуида у правоугаоном каналу под утицајем попречног магнетног поља. На пресеку канала уводи се мали погранични поремећај величине ϵ. Користећи асимптотску анализу у односу на ϵ, добијамо делотворни модел дат експлицитним формулама за брзину и индуковано магнетно поље. Нумерички резултати су потврдили да разматрани поремећаји имају нелокалан утицај на асимптотска решења.

Department of Mathematics
Government First Grade College for Women
Hassan
India
ulavathi@gmail.com

Department of Mathematics
Faculty of Science
University of Zagreb
Zagreb
Croatia
pazanin@math.hr

Department of Mathematics
Faculty of Science
University of Zagreb
Zagreb
Croatia
mradul@math.hr

Departamento de Ecuaciones Diferenciales y Análisis Numérico
Facultad de Matemáticas
Universidad de Sevilla
Sevilla
Spain
fjsgrau@us.es